frontiers | Frontiers in Earth Science

TYPE Original Research
PUBLISHED 20 June 2024
DOI 10.3389/feart.2024.1418087

OPEN ACCESS

EDITED BY
Wenguang Wang,
Northeast Petroleum University, China

REVIEWED BY
Guoqiang Xing,
Changzhou University, China
Mingxian Wang,
Xi'an Shiyou University, China
Lin Du,
University of Alberta, Canada

*CORRESPONDENCE
Lin Cao,
shenglizhiguang123@163.com

RECEIVED 16 April 2024
ACCEPTED 03 June 2024
PUBLISHED 20 June 2024

CITATION
Meng F, Cao L, Zhou Y, Liu B, Wen C and Liu J (2024), Experimental and numerical studies on CO_2 injectivity in low permeability oil reservoirs.
Front. Earth Sci. 12:1418087.
doi: 10.3389/feart.2024.1418087

Experimental and numerical studies on CO_2 injectivity in low permeability oil reservoirs

Fankun Meng[1,2,3], Lin Cao[1,2]*, Yuhui Zhou[1,2,3], Botao Liu[4], Chengyue Wen[1,2] and Jia Liu[1,2]

[1]Key Laboratory of Drilling and Production Engineering for Oil and Gas, Wuhan, China, [2]School of Petroleum Engineering, Yangtze University, Wuhan, China, [3]Western Research Institute, Yangtze University, Karamay, China, [4]School of Computer Science, Yangtze University, Jingzhou, China

Introduction: Contrary to the traditional recognition that CO_2 has large injectivity (the ratio of CO_2 injection volume to pressure drop) in low permeability oil reservoirs to keep the formation pressure at a high level, the CO_2 injection rate usually cannot attain the set value. It is essential to study the factors that influence CO_2 injectivity and propose the optimal strategies to improve the CO_2 injectivity.

Methods: Therefore, in this study, several core samples collected from low permeability oil reservoirs are used to experimentally investigate the influences of CO_2 injection rate, formation permeability, pressure and water saturation on CO_2 injectivity, and the corresponding pressure drop, oil and gas production are examined. To determine the primary factor that influences the CO_2 injectivity, orthogonal experimental design (ODE) and numerical simulations are utilized. In addition, to improve CO_2 injectivity, the techniques of mini-fracturing and radial perforation are presented, and the threshold values for these two parameters are determined.

Result and discussion: The results demonstrate that according to the magnitude of the extent that influences CO_2 injectivity, the rank for the above factors is CO_2 injection rate, reservoir pressure, formation water saturation and permeability. The oil recovery is mainly influenced by CO_2 injection rate and formation permeability, and the influences of reservoir pressure and water saturation on oil recovery are smaller. The threshold values for radial perforation and fracture half-length are 25 m and 50m, respectively, which can provide some guidance for the strategies that should be taken to improve the CO_2 injectivity and recover more oil from low permeability oil reservoirs.

KEYWORDS

CO_2 injectivity, low permeability oil reservoir, CO_2 flooding, experimental study, numerical simulation

1 Introduction

Plenty of laboratory experiments and field pilot tests show that CO_2 flooding can enhance oil recovery significantly. According to the magnitude of formation pressure and minimum miscible pressure (MMP), there are two typical flooding types, miscible flooding and immiscible flooding (Dong et al., 2019). In the condition of miscible flooding, CO_2 can mix with the oil phase easily, which reduces the oil viscosity and density greatly, and the displacement efficiency is much higher than the immiscible flooding (Liu et al., 2020;

Wang et al., 2020). In addition, the effects of CO_2 viscous fingering and gas override are weakened largely (Singh, 2018). Therefore, to improve CO_2 sweep efficiency and oil recovery, CO_2 miscible flooding should be utilized preferentially. To keep the condition of miscible flooding, the formation pressure should be larger than the MMP, and the amount of injected CO_2 should be increased as large as possible. However, in some low permeability oil reservoirs, the CO_2 injection rate cannot attain the set value, which causes the rapid decline of formation pressure, and the status gradually changes from miscible to immiscible flooding. Hence, it is significant to study the primary factors that influence the CO_2 injectivity, and to present the optimal strategies that improve the CO_2 injectivity.

As there are complex fluid distribution patterns, more researches focused on the abnormality of CO_2 injectivity during the water-alternating-gas/CO_2 (WAG) process. Experimentally, the effect of some primary features, such as relative permeability, water saturation, WAG ratio and CO_2 slug size, on CO_2 and bring injectivity during WAG flooding were studied and analyzed (Prieditis et al., 1991; Kamath et al., 1998; Shen et al., 2010; Yang et al., 2015). As the laboratory experiments are complicated and time-consuming, analytical or numerical methods are always used to evaluate the WAG injectivity. Some simple analytical models were developed to analyze the reasons that result in the differences of laboratory- and filed-observed CO_2 tertiary injectivity (Christman and Gorell, 1990; Meng et al., 2018; Meng et al., 2020). Nevertheless, for analytical models, it is difficult to consider some complex effects, such as phase behavior, dispersive mixing, gravity, viscous instability and crossflow. Therefore, numerical simulators are widely utilized to study the impact of these factors on WAG injectivity (Jr et al., 1992; Jr et al., 1992; Faisal et al., 2009; Qiao et al., 2016). For the factors that affect WAG injectivity (John and Rogers, 2001), summarized that wettability, chemical effects, entrapment, relative permeability, saturation effects, interfacial tension (IFT), formation heterogeneity, anisotropy, and stratification have significant impacts on the injectivity.

In analogy to the abundant studies on the injectivity during WAG flooding, the evaluation of CO_2 injectivity during CO_2 sequestration has been researched comprehensively. In terms of the factors that affect CO_2 injectivity (Sokama-Neuyam et al., 2017), found that the fines mobilization can seriously impair CO_2 injectivity in sandstone cores, which is more important than salt precipitation. In addition, the effects of SO_2 as an impurity, irreducible water saturation in a near-well region, non-Darcy flow, phase miscibility and gas compressibility on CO_2 injectivity in sandstone saline aquifer also have been investigated (Mijic et al., 2014; Raza et al., 2015; Wang et al., 2016; Parka et al., 2019). To select the suitable sites for CO_2 storage, and determine the CO_2 injectivity and storage capacity for these sites, some reactive transport models, which consider salt precipitation, and CO_2-water-rock geochemical reactions, were established properly (Xie et al., 2016; Dai et al., 2017; Cui et al., 2018). However, during the CO_2 injection process, several CO_2 storage reservoirs exhibit insufficient formation properties to support commercial-scale injection. Therefore, the application of hydraulic fracturing to enhance CO_2 injectivity was explored, which could significantly increase the CO_2 injection rate and reduce the well bottom-hole pressure (Raziperchikolaee et al., 2013; Huerta et al., 2020; Jung et al., 2020).

According to the above comprehensive reviews about CO_2 injectivity, we can see that the factors that cause the abnormality of CO_2 and water injectivity during WAG flooding have been investigated sufficiently. However, few studies pay attention to the evaluation of CO_2 injectivity during CO_2 flooding in low permeability oil reservoirs. Furthermore, specific measures to improve CO_2 injectivity have not been presented. Although the method of hydraulic fracturing has been implemented to enhance CO_2 injectivity during CO_2 sequestration, there are many differences between CO_2 flooding in low permeability oil reservoirs and CO_2 storage in saline aquifers. Hence, firstly, this paper studies the principal factors that influence CO_2 injectivity during CO_2 flooding in low permeability oil reservoirs through an experimental approach. Then, with the numerical simulation and ODE methods, the primary factors that affect CO_2 injectivity are ranked. Finally, the threshold values for two measures, mini-fracturing and radial perforation are determined, which could provide some guidance for the practical operations.

2 Experimental

2.1 Materials

The core, oil and brine samples are collected from a low permeability oil reservoir in the Shengli oil field. The measured size, porosity and permeability for eight cores are shown in Table 1. In addition, the pore volume (PV) of cores is also calculated. As can be seen, for all of the cores, the permeability is lower than 10 mD, whereas the porosity is almost the same.

For oil samples, through the PVT experiments, the viscosity and density for live oil are measured to be 2.46 mPas and 0.7914 g/cm^3 at the initial reservoir pressure 43.6 MPa and the reservoir temperature 126°C. The measured bubble-point pressure is 10.2 MPa, and the oil-gas ratio and formation volume factor are 37.6 and 1.144, respectively. With the slim-tube displacement tests, the MMP of the oil sample utilized in experiments is 28.9 MPa under reservoir temperature. The detailed compositional analysis for the oil sample is shown in Table 2. It can be seen that the oil samples mainly consist of light or medium components, particularly for C_1, which accounts for 14.77%, while the mole fraction of heavy component C_{11+} is only 27.19%. The measured molecular weight for C_{11+} is 313 g/mol.

For formation brine, the total salinity is 62428 mg/L, and the concentrations for Chloride, Sodium/Potassium are 37764 mg/L and 20617 mg/L. Then, according to the measured results, the salinity of synthetic brine for core experiments could be prepared.

2.2 Experimental setup

Figure 1 shows a schematic of the laboratory experimental setup utilized in this study. In this experimental set-up, there are five subsystems, which include the pump system, storage system, displacement system, monitoring system and temperature control system. For the fluid pump system, on the one hand, the fluids of oil, synthetic water and CO_2 are injected into the core sample under constant injection rate with a syringe pump, on the other hand, the nitrogen with high pressure is used to support the overburden pressure to the core holder. The back pressure at the outlet is set to be greater than the critical pressure of CO_2 (7.39 MPa), which can make the CO_2 keep in a supercritical state. In the monitoring system,

TABLE 1 Measured size, porosity and permeability for collected cores.

No.	Diameter/cm	Length/cm	Permeability/mD	Porosity/%	Pore volume (PV)/cm^3
1	2.5	20	5.2	16.6	16.3
2	2.5	20	5.6	16.3	16.0
3	2.5	20	8.1	17.4	17.1
4	2.5	20	8.2	17.5	17.2
5	2.5	20	5.8	16.8	16.5
6	2.5	20	5.6	16.3	16.0
7	2.5	20	2.5	16.0	15.7
8	2.5	20	0.63	15.8	15.5

TABLE 2 Components of oil sample with compositional analysis.

Component	Mole fraction/%	Component	Mole fraction/%
CO_2	0.98	C_5	3.41
C_1	14.77	C_6	11.65
C_2	1.71	C_7	10.53
C_3	2.85	C_8	8.17
IC_4	0.63	C_9	6.97
C_4	3.34	C_{10}	4.97
IC_5	2.83	C_{11+}	27.19

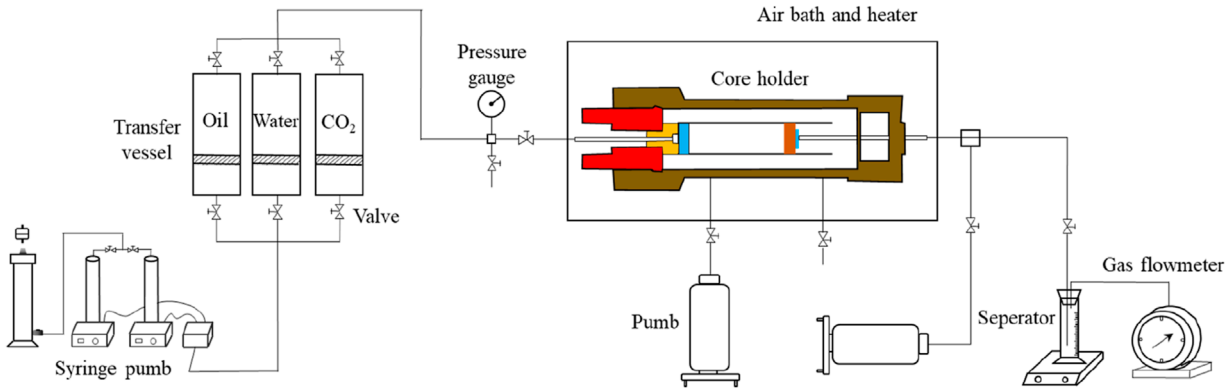

FIGURE 1
Schematic of the experimental setup for CO_2 flooding.

the CO_2 injection pressure, the produced oil and gas, are measured with pressure gauge, liquid collector, and gas flow meter, respectively. With the temperature control system, the experiment temperature is maintained at reservoir temperature.

2.3 Experimental procedure

The factors that affect CO_2 injectivity could be classified into geological features and production parameters. In this experimental

TABLE 3 Core sample specifications and designed parameters for four scenarios.

Scenario	Core no.	Original oil in place (OOIP)/cm^3	Connate water saturation	Production pressure/MPa	Injection rate/(cm^3/min)	Formation permeability/mD
#1	1	9.5	0.42	20	0.1	5.2
	2	7.5	0.53	20	0.05	5.6
#2	3	10	0.41	20	0.01	8.1
	4	10.5	0.39	10	0.01	8.2
#3	5	9.5	0.42	20	0.01	5.8
	6	5	0.69	20	0.01	5.6
#4	7	9.5	0.40	20	0.01	2.5
	8	9.8	0.37	20	0.01	0.63

study, the effects of four primary factors on CO_2 injectivity and oil recovery, which are CO_2 injection rate, formation pressure, water saturation, and formation permeability, are investigated. Some scholars had also studied these four parameters. The presence of residual natural gas saturation, in the short term, would decrease the CO2 injectivity considerably. However, with a permeability dependent rate, the situation would improve as more natural gas is recovered (Saeedi and Rezaee, 2012). In addition, it would be wised to evaluate injectivity experimentally or numerically by considering the residual constraints (fraction of water, remaining gas, and condensate (oil phase)) as it varies with the injection rates, formation pressure (Raza A., et al., 2017; Lzgec O., et al., 2008). However, to further investigate the effect of these four parameters on CO_2 injectivity, four scenarios are designed reasonably, and the detailed information of used cores in each scenario is listed in Table 3. The introduction for each scenario is shown as follows.

(1) **Scenario #1.** CO_2 is injected into the two core samples with similar porosity, permeability and connate water saturation at rates of 0.1 mL/min and 0.05 mL/min.
(2) **Scenario #2.** The production pressure is set to be 20 MPa and 10 MPa for two core samples with similar porosity, permeability and connate water saturation.
(3) **Scenario #3.** Two core samples with similar porosity and permeability, whose connate water saturation are 0.42 and 0.69, are selected and used to conduct CO_2 flooding.
(4) **Scenario #4.** Two core samples with similar porosity and connate water saturation, whose formation permeability are 2.5 mD and 0.63 mD, are employed to conduct CO_2 flooding.

The experimental procedure is as follows.

Step 1: to simulate the oil reservoir under the initial condition, the core samples should be evacuated with a vacuum pump before the implementation of CO_2 flooding.
Step 2: synthetic water is injected into the cores at different rates. Subsequently, the core samples are flooded with live oil at a constant rate until there is no water production. Thus, the irreducible water saturation (connate water saturation) and original oil in place (OOIP) for each core sample can be acquired, which is shown in Table 3.
Step 3: The production pressure is set to be 20 MPa, which makes it identical to the current formation pressure.
Step 4: During the CO_2 flooding process for these four scenarios, the pressure drop, gas production and oil production are measured. Then, the oil recovery and CO_2 injectivity are calculated. In this study, CO_2 injectivity is defined as the ratio of CO_2 injection rate to a measured pressure drop. Once the CO2 flooding is terminated, by reducing the backpressure in a stepwise manner, the system pressure could be reduced to the atmospheric pressure.

3 Experimental results and discussion

3.1 CO_2 injection rate (scenario #1)

Scenario #1 evaluates the effects of CO_2 injection rate on CO_2 injectivity. For different CO_2 injection rates, the oil recovery and cumulative gas production versus injected volume are shown in Figure 2, and the pressure drop and CO_2 injectivity versus injected volume are shown in Figure 3. As can be seen from these two figures, in the beginning, the CO_2 is compressed and injected into the core sample, in this stage, the injection pressure drop increase, and there is no oil production. It is obvious that the ultimate oil recovery and pressure drop increase with injection rate, while the gas breakthrough time and CO_2 injectivity in the later period decrease with it. The reasons for this phenomenon can be attributed to the fact that a larger CO_2 injection rate can greatly increase formation pressure, which increases the miscibility between CO_2 and oil and reduces the moving velocity of the CO_2 displacement front. Due to the better miscibility under a high CO_2 injection rate (0.1 cc/min), thus the swept efficiency of CO_2 and oil recovery are improved, and after CO_2 breakthrough the CO_2 injectivity

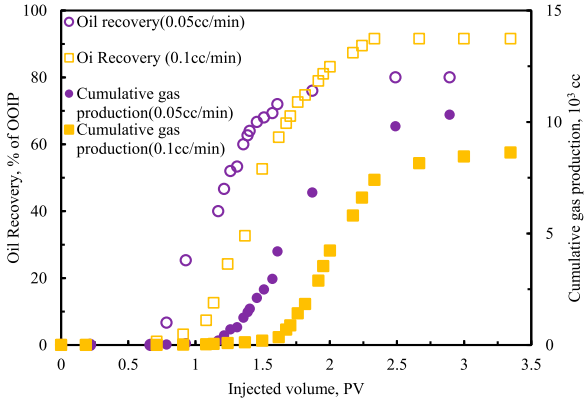

FIGURE 2
Measured oil recovery, cumulative gas production versus CO_2 injected volume.

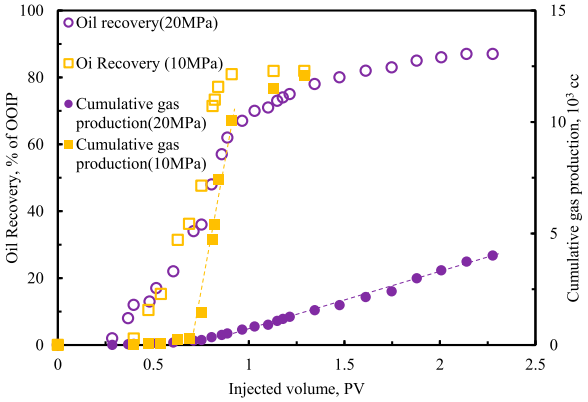

FIGURE 4
Measured oil recovery, cumulative gas production versus CO_2 injected volume.

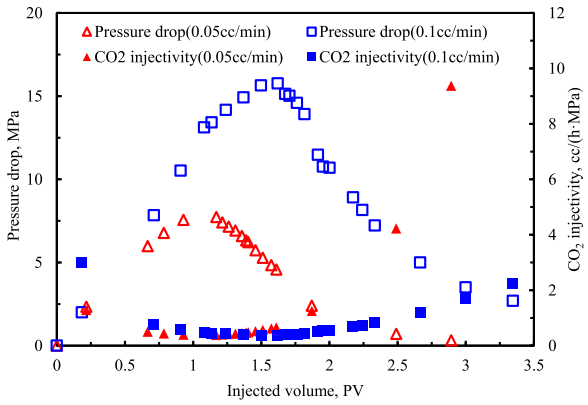

FIGURE 3
Measured injection pressure drop, calculated CO_2 injectivity versus CO_2 injected volume.

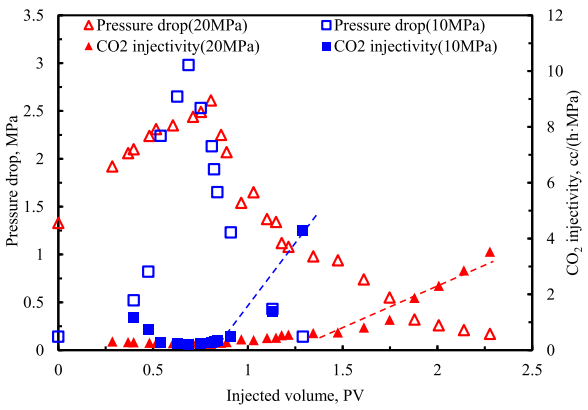

FIGURE 5
Measured injection pressure drop, calculated CO_2 injectivity versus CO_2 injected volume.

is much lower than the injectivity under a small CO_2 injection rate (0.05 cc/min).

3.2 Formation pressure (scenario #2)

The influences of formation pressure on CO_2 injectivity are studied in scenario #2. Figure 4 and Figure 5 show the oil recovery and cumulative gas production versus injected volume, the pressure drop and CO_2 injectivity versus injected volume, respectively. Since a larger formation pressure can increase the miscibility of CO_2 and oil, then as shown in Figure 4, the growth rate of cumulative gas production for this case is less than the case with lower formation pressure, and the ultimate oil recovery is higher. As the CO_2 injection rate is the same for both cases, the gas breakthrough time, maximum pressure drop and injectivity are almost identical. Nevertheless, with the decline of pressure drop, the CO_2 injectivity increases gradually. Since on the condition of large formation pressure, the mixing of CO_2 and oil is sufficient, thus the rising rate of CO_2 injectivity is less than the case with lower formation pressure.

3.3 Formation water saturation (scenario #3)

Under the different water saturation conditions, Figure 6 and Figure 7 plot the measured oil recovery, cumulative gas production versus CO_2 injected volume and measured pressure drop, calculated CO_2 injectivity versus CO_2 injected volume, respectively. As shown in these two figures, for the case with higher water saturation, the maximum values of cumulative gas production and pressure drop are significantly less than the case with lower saturation, which also causes the CO_2 injectivity for the former case to be larger than the latter case. Through the comprehensive analysis for the above phenomenon, it can be speculated that with high water saturation, CO_2 flooding is similar to carbonated water or WAG displacement, thus CO_2 mobility is greatly reduced, and CO_2

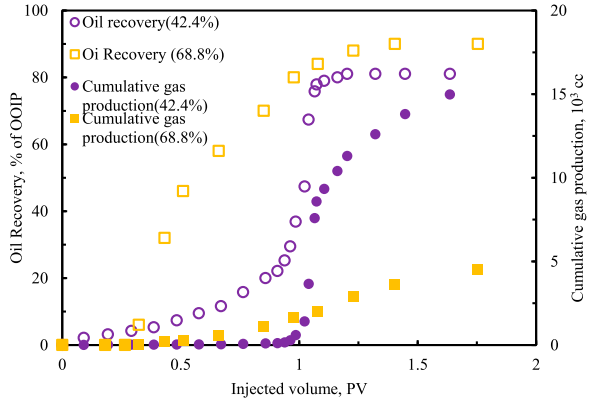

FIGURE 6
Measured oil recovery, cumulative gas production versus CO_2 injected volume.

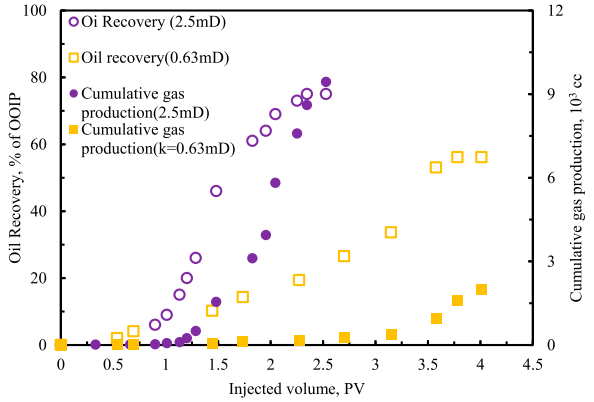

FIGURE 8
Measured oil recovery, cumulative gas production versus CO_2 injected volume.

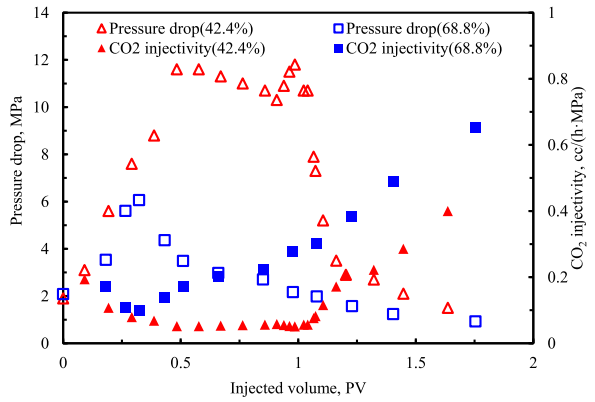

FIGURE 7
Measured injection pressure drop, calculated CO_2 injectivity versus CO_2 injected volume.

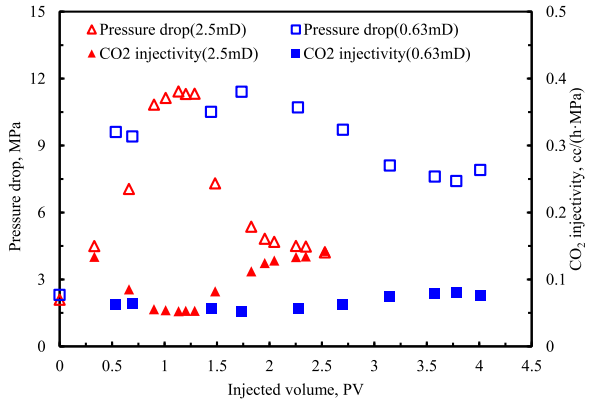

FIGURE 9
Measured injection pressure drop, calculated CO_2 injectivity versus CO_2 injected volume.

swept efficiency is improved. In addition, influenced by the capillary trapping effect for cases with high water saturation, a large amount of CO_2 is trapped in the porous media, which results in the decline of gas production. Since the mobility of oil is much lower than the water, the CO_2 injectivity in the formation with low water saturation is less than the formation with high water saturation.

3.4 Formation permeability (scenario #4)

For core samples with different permeability, Figure 8 shows the oil recovery, gas production versus CO_2 injected volume, and Figure 9 shows the injection pressure drop, CO_2 injectivity versus CO_2 injected volume. As the porous space for formation with lower permeability is mainly consisted of micro and nanopores, the CO_2 moving velocity in these pores is slower, and a large number of CO_2 is trapped in the micropores, which causes that the rising rate of oil recovery and gas production is lower, as shown in Figure 2. To obtain a higher oil recovery, more CO_2 is needed for tight formation in practice. Furthermore, impacted by the large portion of micro and nanopores, the CO_2 injectivity for tight formation is significantly less than the formation with larger permeability.

4 Numerical simulation

As shown in the above parts, the factors that influence the CO_2 injectivity have been studied through experiments; however, due to the complexity and time-consuming of experiments, it is difficult to evaluate the influence of these factors on CO_2 injectivity quantitatively. Therefore, the combinations of numerical simulation and OED methods are used to solve the mentioned problems.

4.1 Basic model

The oil reservoir of interest is located in Bohai Bay Basin, Shengli oilfield, which has 19 production wells and 11 injection wells in total. As can be seen from Figure 10A that there are many

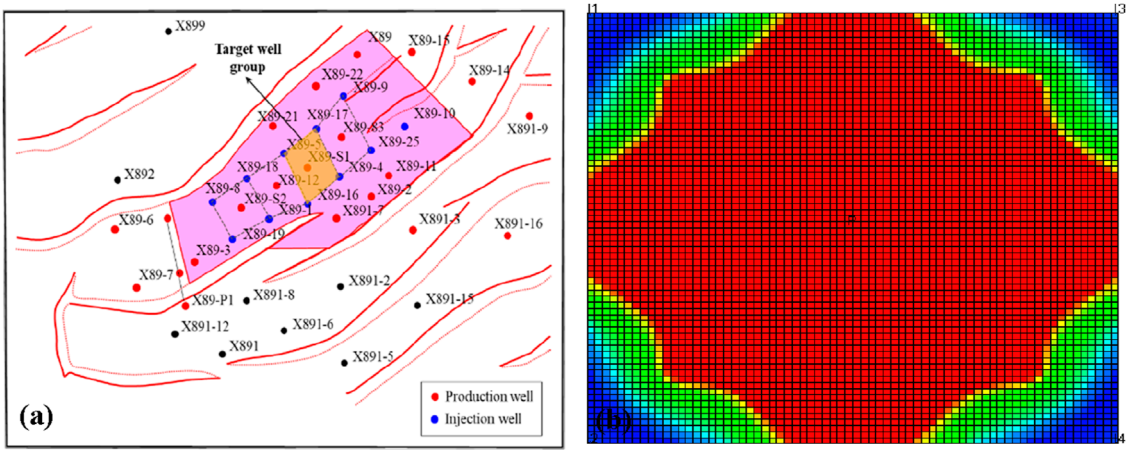

FIGURE 10
(A) Well locations in the reservoir of interest and **(B)** the presented model in this paper.

TABLE 4 Formation and production parameters for target well group.

Parameters	Values	Parameters	Values
Well space/m	350	Rock compressibility factor/MPa^{-1}	2.6×10^{-4}
Formation thickness/m	10.6	CO_2 injection rate/(sm^3/d)	254.5
Porosity/%	13	Oil production rate (depleted exploitation)/(m^3/d)	1.65
Permeability/mD	4.7	Oil production rate (CO_2 flooding)/(m^3/d)	3.3
Reservoir datum depth/m	2950	CO_2 diffusion coefficient/(m^2/d)	0.589
Reservoir temperature/°C	126	Depleted exploitation period/yr	5
Initial reservoir pressure/MPa	42.6	CO_2 flooding period/yr	10

faults in this reservoir, which belongs to a complex fault-block oil formation. Currently, CO_2 flooding is only implemented in the main body of this reservoir, and the well group is a classical five-point pattern. To evaluate the CO_2 injectivity of injection wells and the production performance of production wells directly, one of the well groups is selected, and the detailed information about formation and production parameters is shown in Table 4. The fluid compositional components are shown in Table 2. With Eclipse compositional simulator, a grid system of 70 × 70 × 5 is developed and represented the target well group, which results in a grid block size of 5 × 5 × 2.12 m, as shown in Figure 10B.

Initially, the depleted development is adopted, and after 5 years of depleted production, CO2 flooding is used to enhance oil recovery in the low permeability reservoir. The relative permeability curves for oil/gas phases and oil/water phases used in this study are shown in Figure 11, which are acquired from the laboratory experiments. The measurement process of the relative permeability curve for oil/water phases and oil/gas phases is as follows:

The oil and water are injected into the core at a certain flow rate at the same time, which creates a pressure difference at both ends of the core. When the oil/water flow rate are stable, the oil/water saturations in the core do not change. According to Darcy's law, the permeabilities of the oil/water phases at a certain saturation are calculated. By changing the oil/water flow ratio, the permeabilities of the oil/water phases under different saturations can be calculated, and then the relative permeability curve for oil/water phases can be drawn. The same is true for the relative permeability curve of gas and oil.

4.2 Orthogonal experimental design (OED)

To evaluate the influences of four factors (CO_2 injection rate, formation pressure, water saturation, and permeability) mentioned in the experimental study quantitatively, the OED method is employed. According to a practical variation range for injection rate, formation pressure, reservoir water saturation, and rock permeability, the levels for these parameters are designed reasonably, which are shown in Table 5.

Since there are four factors, thus orthogonal array L_9 (3^4) is used to design the schemes, which is shown in Table 6. For each scheme, through the application of the numerical simulator,

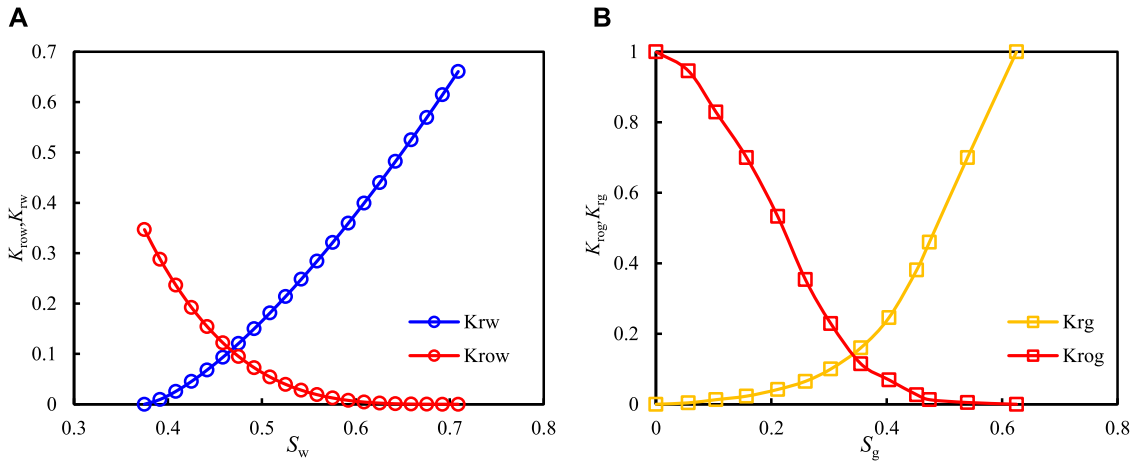

FIGURE 11
Relative permeability curves for **(A)** oil-water phase and **(B)** oil-gas phase.

TABLE 5 Design of levels for four primary influential factors.

Level	CO_2 injection rate/(m^3/d)	Formation pressure/MPa	Water saturation/%	Formation permeability/mD
1	300	42.6	37.5	2.5
2	350	37.6	40	5
3	400	32.6	42.5	7.5

the production performances for the reservoir and wells can be obtained. The other essential parameters during the simulation can be found in Section 4.1. In Table 6, the CO_2 injectivity is defined as the ratio of total CO_2 injection volume to formation pressure drop. The used pressure drop is the difference between the formation average pressure in the last moment and the value before CO_2 flooding.

According to the numerical simulation results, the mean value for each level can be calculated, which is expressed as K_1, $K_2$and K_3in Table 7. In addition, the range for each level, R, can also be obtained.

It can be seen from Table 7 that the range R for different CO_2 injection rate is the largest (342.1 t/MPa), while for formation permeability it is the lowest (107.5 t/MPa), which indicates that CO_2 injectivity is primarily influenced by CO_2 injection rate, and the formation permeability has few effects on CO_2 injectivity. The formation water saturation and permeability have moderate impacts on CO_2 injectivity. The results are identical to experimental observations. For instance, through the comparisons of Figures 3, 5, 7, and 9, we can see that the difference of maximum CO_2 injectivity for different injection rates is largest, which is 7.15 cc/(hMPa). Whereas the difference of maximum injectivity for different permeability is 0.07 cc/(hMPa), which is lower than the other factors. For different formation pressure and water saturation, the differences of maximum injectivity are 0.76 cc/(hMPa) and 0.25 cc/(hMPa), respectively, which are intermediate between the injection rate and formation permeability. Therefore, through the combination of OED results and experimental observations, we can conclude that the rank for the influential factors of CO_2 injectivity is CO_2 injection rate, reservoir pressure, formation pressure, and permeability.

4.3 CO_2 injectivity improvement strategies

As mentioned above, the CO_2 injection rate is the primary factor that affects CO_2 injectivity, therefore, reasonable measures that can improve the CO_2 injection rate should be presented. In this study, two measures are proposed, which are radial perforation and mini-fracturing. The locations of radial perforation wellbore and mini-fractures are shown in Figure 12. To simulate the mini-fractures properly, Local Grid Refinement (LGR) technology is utilized, and the refined grids conform to the logarithmic distribution pattern.

On the one hand, the employment of radial perforation and mini-fracturing can enhance the CO_2 injectivity, on the other hand, the implementation of radial perforation and mini-fracturing can result in the appearance of gas channeling in advance. To obtain large CO_2 injectivity and avoid the early gas breakthrough simultaneously, the lengths for radial perforation and mini-fracturing should be optimized. The parameters that are used have been listed in Section 4.1.

4.3.1 Radial perforation

Figure 13 plots the relationship curve between radial perforation length and CO_2 injectivity. The method to calculate CO_2 injectivity

TABLE 6 Orthogonal design schemes and simulation results.

Schemes	CO_2 injection rate/(m^3/d)	Formation pressure/MPa	Formation water saturation/%	Formation permeability/mD	CO_2 injectivity/(t/MPa)
1	300	42.6	37.5	2.5	551.8
2	300	37.6	40	5	845.0
3	300	32.6	42.5	7.5	431.8
4	350	42.6	40	7.5	658.9
5	350	37.6	42.5	2.5	392.1
6	350	32.6	37.5	5	195.8
7	400	42.6	42.5	5	429.3
8	400	37.6	37.5	7.5	169.1
9	400	32.6	40	2.5	203.8

TABLE 7 Analysis for the simulation results of designed schemes.

	CO_2 injectivity for different injection rate/(t/MPa)	CO_2 injectivity for different formation pressure/(t/MPa)	CO_2 injectivity for different formation water saturation/(t/MPa)	CO_2 injectivity for different formation permeability/(t/MPa)
K_1	609.5	546.7	305.6	382.6
K_2	415.6	468.7	569.2	490.0
K_3	267.4	277.1	417.7	419.9
R	**342.1**	**269.5**	**263.7**	**107.5**

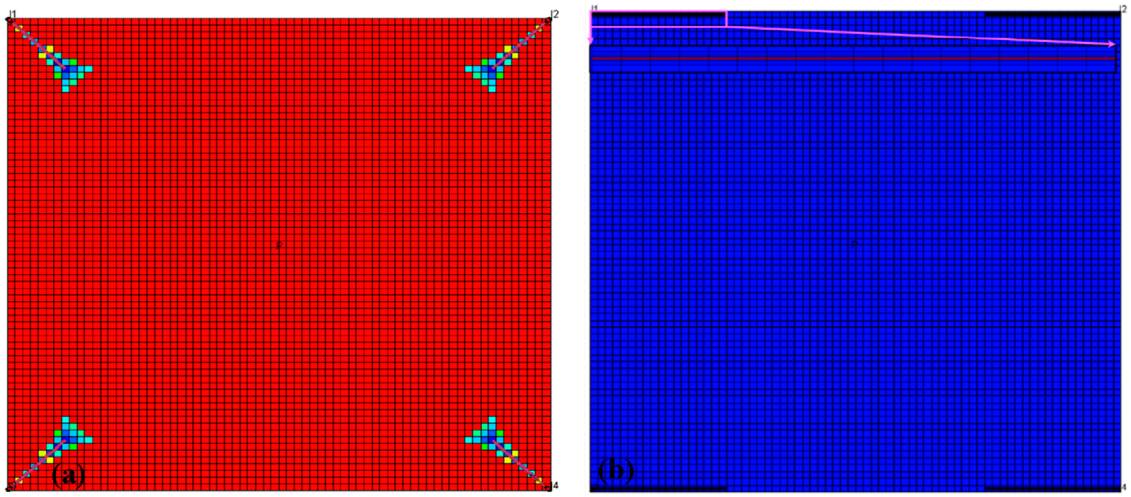

FIGURE 12
Numerical simulation models for **(A)** radial perforation and **(B)** mini-fracturing measures.

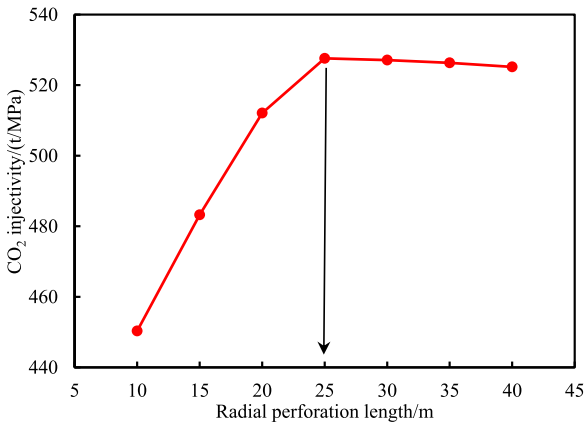

FIGURE 13
Relationship between radial perforation length and CO_2 injectivity.

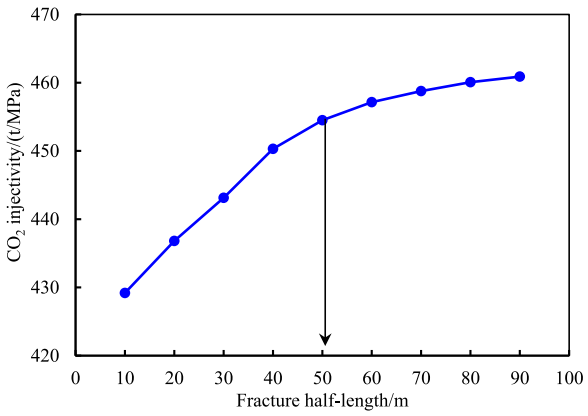

FIGURE 14
Relationship between mini-fracture half-length and CO_2 injectivity.

has been stated in Section 4.2. It can be seen from this figure that when the radial perforation length is less than 25 m, the CO_2 injectivity increases with the radial perforation length; when it is larger than 25 m, the CO_2 injectivity for different radial perforation lengths is nearly the same, which demonstrates that the threshold value for radial perforation length is 25 m. The reasons for this phenomenon may be attributed to the fact that on the condition of identical injection volume for different radial perforation lengths, when it is lower than one certain value, the formation energy cannot be supplemented in time. However, when it is larger than this critical value, the formation energy can be supplemented, and the rise of radial perforation length has few effects on the CO_2 injectivity.

4.3.2 Mini-fracturing

The relationship between mini-fracture half-length and CO_2 injectivity is shown in Figure 14. As can be seen from this figure, in the beginning, the CO_2 injectivity increases with min-fracture half-length drastically. Nevertheless, when the half-length is larger than 50 m, the increasing rate of CO_2 injectivity decline obviously. Therefore, it can be concluded that the threshold value for min-fracture half-length is 50 m in this study. In addition, it can be seen that the relationship curves in Figure 13 and Figure 14 are similar, which indicates that the reasons for interpreting the variation rule are also the same as each other.

5 Conclusion

This paper studies the factors that affect CO_2 injectivity and oil recovery through the experiments. With the numerical simulation and OED method, the rank for primary factors that influence CO_2 injectivity is given, and the optimal radial perforation length and mini-fracture half-length are presented. Some highlights of this work include the following.

(1) CO_2 injection has the largest impact on CO_2 injectivity, while the formation permeability has the lowest influence on CO_2 injectivity, and the formation saturation and pressure are intermediate between the CO_2 injection and formation permeability.
(2) For formation with large water saturation, the injectivity and displacement efficiency is higher, while the gas production is lower, which indicates that it is more suitable for the implementation of CO_2 flooding and sequestration.
(3) On the condition of large formation pressure, due to the sufficient solution and diffusivity of oil and CO_2, the gas production is less, and the CO_2 injectivity increases gradually, which indicates that the earlier CO_2 flooding is implemented, the better production performance can be obtained.
(4) To enhance CO_2 injectivity, the measures of radial perforation and mini-fracturing can be taken, and the threshold values for the perforation length and the fracture half-length are 25 m and 50 m, respectively.

Data availability statement

The raw data supporting the conclusion of this article will be made available by the authors, without undue reservation.

Author contributions

FM: Writing–review and editing. LC: Writing–original draft. YZ: Resources, Project administration, Software, Writing–review and editing. BL: Writing–original draft, Resources, Supervision. CW: Conceptualization, Data curation, Formal Analysis, Writing–original draft. JL: Investigation, Methodology, Software, Validation, Writing–review and editing.

Funding

The author(s) declare that financial support was received for the research, authorship, and/or publication of this article. This work is supported by the National Natural Science Foundation of China (Grant No. 52104018, 52274030).

Acknowledgments

The authors would like to appreciate reviewers and editors whose critical comments were helpful in preparing this article.

Conflict of interest

The authors declare that the research was conducted in the absence of any commercial or financial relationships that could be construed as a potential conflict of interest.

Publisher's note

All claims expressed in this article are solely those of the authors and do not necessarily represent those of their affiliated organizations, or those of the publisher, the editors and the reviewers. Any product that may be evaluated in this article, or claim that may be made by its manufacturer, is not guaranteed or endorsed by the publisher.

References

Christman, P. G., and Gorell, S. B. (1990). Comparison of laboratory-and field-observed CO_2 tertiary injectivity. *J. Petroleum Technol.* 42 (2), 226–233. doi:10.2118/17335-pa

Cui, G., Wang, Y., Rui, Z., Chen, B., Ren, S., and Zhang, L. (2018). Assessing the combined influence of fluid-rock interactions on reservoir properties and injectivity during CO_2 storage in saline aquifers. *Energy* 155, 281–296. doi:10.1016/j.energy.2018.05.024

Dai, Z., Zhang, Y., Stauffer, P., Xiao, T., Zhang, M., Ampomah, W., et al. (2017). Injectivity evaluation for offshore CO_2 sequestration in marine sediments. *Energy Procedia* 114, 2921–2932. doi:10.1016/j.egypro.2017.03.1420

Dong, P., Liao, X., Chen, Z., and Chu, H. (2019). An improved method for predicting CO_2 minimum miscibility pressure based on artificial neural network. *Adv. Geo-Energy Res.* 3 (4), 355–364. doi:10.26804/ager.2019.04.02

Faisal, A., Bisdom, K., Zhumabek, B., Mojaddam Zadeh, A., and Rossen, W. R. (2009). "Injectivity and gravity segregation in WAG and SWAG enhanced oil recovery," in *Paper presented at SPE annual technical conference and exhibition*, 4–7.

Huerta, N. J., Cantrell, K. J., White, S. K., and Brown, C. F. (2020). Hydraulic fracturing to enhance injectivity and storage capacity of CO_2 storage reservoirs: benefits and risks. *Int. J. Greenh. Gas Control* 100 (1013105), 103105–103112. doi:10.1016/j.ijggc.2020.103105

Izgec, O., Demiral, B., Bertin, H., and Akin, S. (2008). CO_2 injection into saline carbonate aquifer formations I: laboratory investigation. *Transp. Porous Media* 72 (1), 1–24. doi:10.1007/s11242-007-9132-5

JohnRogers, D. R. B. G., and Grigg, R. B. (2001). A literature analysis of the WAG injectivity abnormalities in the CO_2 process. *SPE Reserv. Eval. Eng.* 4 (5), 375–386. doi:10.2118/73830-pa

Jr, M. K. R., Cheng, C. T., Varnon, J. E., Pope, G. A., and Sepehrnoori, K. (1992). "Interpretation of a CO_2 WAG injectivity test in the San Andres formation using a compositional simulator," in *Paper presented at SPE/DOE eighth symposium on enhanced oil recovery*. Tulsa, Oklahoma, USA.

Jr, M. K. R., Pope, G. A., and Sepehrnoori, K. (1992). "Analysis of tertiaryinjectivity of carbon dioxide," in *Paper presented at SPE permian basin oil and gas recovery conference midland*, 18–20.

Jung, H., Espinoza, D. N., and Hosseini, S. A. (2020). Wellbore injectivity response to step-rate CO_2 injection: coupled thermo-poro-elastic analysis in a vertically heterogeneous formation. *Int. J. Greenh. Gas Control* 102, 103156. doi:10.1016/j.ijggc.2020.103156

Kamath, J., Nakagawa, F. M., Boyer, R. E., and Edwards, K. A. (1998). "Laboratory investigation of infectivity losses during WAG in West Texas Dolomites," in *Paper presented at SPE permian badn oil and gas recovery cofderence, midland,Texas, USA*, 22–27.

Liu, H., Zhu, Z., Patrick, W., Liu, J., Lei, H., and Zhang, L. (2020). Numerical visualization of supercritical CO_2 displacement in pore-scale porous and fractured media saturated with water. *Adv. Geo-Energy Res.* 4 (4), 419–434. doi:10.46690/ager.2020.04.07

Meng, F., Su, Y., Hao, Y., Li, Y., and Tong, G. (2018). Injectivity of CO_2 WAG in low permeability oil reservoirs based on B-L equation. *J. China Univ. Petroleum* 42 (4), 91–99. doi:10.3969/j.issn.1673-5005.2018.04.011

Meng, F., Su, Y., Wang, W., Lei, Q., and He, D. (2020). Semi-analytical evaluation for water-alternating-CO_2 injectivity in tight oil reservoirs. *Int. J. Oil Gas Coal Technol.* 24 (1), 62–84. doi:10.1504/ijogct.2020.106704

Mijic, A., LaForce, T. C., and Muggeridge, A. H. (2014). CO_2 injectivity in saline aquifers: the impact of non-Darcy flow, phase miscibility, and gas compressibility. *Water Resour. Res.* 50 (5), 4163–4185. doi:10.1002/2013wr014893

Parka, Y.-C., Kimb, S., Leec, J. H., and Shinn, Y. J. (2019). Effect of reducing irreducible water saturation in a near-well region on CO_2 injectivity and storage capacity. *Int. J. Greenh. Gas Control* 86, 134–145. doi:10.1016/j.ijggc.2019.04.014

Prieditis, J., Wolle, C. R., and Notz, P. K. (1991). "A laboratory and field injectivity study CO_2 WAG in the San Andres formation of West Texas," in *Paper presented at SPE 66rd annual technical conference and exhibition, Dallas, TX, USA*.

Qiao, C., Li, L., Johns, R. T., and Xu, J. (2016). Compositional modeling of dissolution-induced Injectivity alteration during CO_2 flooding in carbonate reservoirs. *SPE J.* 21 (03), 0809–0826. doi:10.2118/170930-pa

Raza, A., Gholami, R., Rezaee, R., Bing, C. H., Nagarajan, R., and Hamid, M. A. (2017). Preliminary assessment of CO_2 injectivity in carbonate storage sites. *Petroleum* 3 (1), 144–154. doi:10.1016/j.petlm.2016.11.008

Raza, A., Rezaee, R., Gholami, R., Rasouli, V., Bing, C. H., Nagarajan, R., et al. (2015). Injectivity and quantification of capillary trapping for CO_2 storage: a review of influencing parameters. *J. Nat. Gas Sci. Eng.* 26, 510–517. doi:10.1016/j.jngse.2015.06.046

Raziperchikolaee, S., Alvarado, V., and Yin, S. (2013). Effect of hydraulic fracturing on long-term storage of CO_2 in stimulated saline aquifers. *Appl. Energy* 102, 1091–1104. doi:10.1016/j.apenergy.2012.06.043

Saeedi, A., and Rezaee, R. (2012). Effect of residual natural gas saturation on multiphase flow behaviour during CO_2 geo-sequestration in depleted natural gas reservoirs. *J. Petroleum Sci. Eng.* 82-83, 17–26. doi:10.1016/j.petrol.2011.12.012

Shen, P., Chen, X., and Qin, J. (2010). Pressure characteristics in CO_2 flooding experiments. *Petroleum Explor. Dev.* 37 (2), 211–215. doi:10.1016/s1876-3804(10)60026-2

Singh, H. (2018). Impact of four different CO_2 injection schemes on extent of reservoir pressure and saturation. *Adv. Geo-Energy Res.* 2 (3), 305–318. doi:10.26804/ager.2018.03.08

Sokama-Neuyam, Y. A., Ginting, P. U. R., Timilsina, B., and Ursin, J. R. (2017). The impact of fines mobilization on CO_2 injectivity: an experimental study. *Int. J. Greenh. Gas Control* 65, 195–202. doi:10.1016/j.ijggc.2017.08.019

Wang, W., Meng, F., Su, Y., Hou, L., Geng, X., Hao, Y., et al. (2020). A simplified capillary bundle model for CO_2-alternating-water Iinjection using an equivalent resistance method. *Geofluids* 2020, 1–14. doi:10.1155/2020/8836287

Wang, Z., Wang, J., Lan, C., Ko, V., Ryan, D., and Wigston, A. (2016). A study on the impact of SO_2 on CO_2 injectivity for CO_2 storage in a Canadian saline aquifer. *Appl. Energy* 184, 329–336. doi:10.1016/j.apenergy.2016.09.067

Xie, J., Zhang, K., Li, C., and Wang, Y. (2016). Preliminary study on the CO_2 injectivity and storage capacity of low-permeability saline aquifers at Chenjiacun site in the Ordos Basin. *Int. J. Greenh. Gas Control* 52, 215–230. doi:10.1016/j.ijggc.2016.07.016

Yang, D., Song, C., Zhang, J., Ji, Y., and Gao, J. (2015). Performance evaluation of injectivity for water-alternating-CO_2 processes in tight oil formations. *Fuel* 139, 292–300. doi:10.1016/j.fuel.2014.08.033